Extremophiles (2008) 12:719–728
DOI 10.1007/s00792-008-0179-1

ORIGINAL PAPER

Irreversible inhibition of the thermophilic esterase EST2 from *Alicyclobacillus acidocaldarius*

Ferdinando Febbraio · Sandro Esposito D'Andrea · Luigi Mandrich · Luigia Merone · Mosè Rossi · Roberto Nucci · Giuseppe Manco

Received: 22 February 2008 / Accepted: 18 June 2008 / Published online: 12 July 2008

Abstract Kinetic studies of irreversible inhibition in recent years have received growing attention owing to their relevance to problems of basic scientific interest as well as to their practical importance. Our studies have been devoted to the characterization of the effects that well-known acetylcholinesterase irreversible inhibitors exert on a carboxylesterase (EST2) from the thermophilic eubacterium *Alicyclobacillus acidocaldarius*. In particular, sulfonyl inhibitors and the organophosphorous insecticide diethyl-*p*-nitrophenyl phosphate (paraoxon) have been studied. The incubation of EST2 with sulfonyl inhibitors resulted in a time-dependent inactivation according to a pseudo-first-order kinetics. On the other hand, the EST2 inactivation process elicited by paraoxon, being the inhibition reaction completed immediately after the inhibitor addition, cannot be described as a pseudo-first-order kinetics but is better considered as a high affinity inhibition. The values of apparent rate constants for paraoxon inactivation were determined by monitoring the enzyme/substrate reaction in the presence of the inhibitor, and were compared with those of the sulfonyl inhibitors. The protective effect afforded by a competitive inhibitor on the EST2 irreversible inhibition, and the reactivation of a complex enzyme/irreversible-inhibitor by hydroxylamine and 2-PAM, were also investigated. The data have been discussed in the light of the recently described dual substrate binding mode of EST2, considering that the irreversible inhibitors employed were able to discriminate between the two different binding sites.

Keywords *Alicyclobacillus acidocaldarius* · High-affinity inhibition · Thermophilic esterase · Paraoxon · Chemical warfare agents · Enzyme reactivation

Abbreviations

EST2	Esterase 2
HSL	Hormone sensitive lipase
2-PAM	2-(hydroxyiminomethyl)-1-methylpyridinium iodide
Paraoxon	Diethyl-*p*-nitrophenyl phosphate
PMSF	Phenylmethanesulfonyl fluoride
HDSC	1-Hexadecanesulfonyl chloride
*p*NP-C6	Nitrophenyl-hexanoate
*p*NP-C12	Nitrophenyl-dodecanoate
HEPES	2-[4-(2-hydroxyethyl)-1-piperazino]-ethansulfonic acid

Introduction

Irreversible inhibition kinetics is less documented and investigated compared to competitive kinetics. Nevertheless, in the last years it has received growing attention in the literature because of its relevance not only to basic scientific research but also to matters of practical importance. As an example, by using irreversible inhibitors, it is possible to identify the amino acid residues involved in the catalytic mechanism by applying labeling protocols followed by chemical hydrolysis and/or proteolysis,

This work was supported by a grant to G. M. from "Regione Campania" Year 2000.

Communicated by A. Driessen.

F. Febbraio (✉) · S. E. D'Andrea · L. Mandrich · L. Merone · M. Rossi · R. Nucci · G. Manco
Istituto di Biochimica delle Proteine, CNR,
Via P. Castellino 111, 80131 Naples, Italy
e-mail: f.febbraio@ibp.cnr.it

associated with mass spectrometry techniques (Legler and Harder 1978; Tull et al. 1991; Febbraio et al. 1997; Manco et al. 1999). Moreover, the crystallographic analysis of enzyme-complexes with irreversible inhibitors that mimic the reaction intermediates has provided essential information on the mechanisms of enzymatic catalysis (Withers and Aebersold 1995; De Simone et al. 2000, 2004a). As far as applications are concerned, irreversible inhibition is employed in the inactivation of enzymes with harmful properties (Lu et al. 2007; Demo et al. 2007; Hugonnet and Blanchard 2007; Bhat et al. 2008) or, sometimes, it is involved in key vital processes such as the action of pesticides on acetylcholinesterases for pest and insect control (Maklakov et al. 2001; Zdrazilová et al. 2006).

Irreversible inhibition differs from reversible inhibition in the formation of a covalent adduct between the reactive functional groups of the inhibitor and the active site amino acid side chain. Usually, an irreversible inhibition denotes that all attempts to remove the inhibiting group by chemical means have been unsuccessful, although the possibility is not thereby excluded that the inhibition may become reversible as the result of supplementary work. In this case, it is more correct to use the term "reactivation" rather than "reversal" for such a chemical removal of the inhibiting group (Dixon and Webb 1979). Irreversible inhibition is characterized by a progressive increase over time, ultimately reaching complete inhibition, even with a very dilute inhibitor, provided that the inhibitor is in excess of the enzyme present.

Thus, the conventional method of (pseudo) rate-constant determination in irreversible inhibition foresees a time-dependent activity assay of an enzyme/inhibitor mixture, with the simplification that the quantity of the inhibitor is significantly greater than that of the enzyme, so that pseudo first-order conditions apply (Legler and Harder 1978; Dixon and Webb 1979). Nevertheless, this method is not easily applicable to the study of fast rate inhibitions with a reaction time of less than few seconds.

Some years ago, in an attempt to obtain values of apparent rate constants for irreversible high-affinity inhibition, the same concepts of reversible inhibition were proposed as applicable to such inhibition (Liu and Tsou 1986). In particular, it was possible to obtain values of apparent rate constants for inactivation by monitoring the enzyme/substrate reaction in the presence of the inhibitor, according to Leytus et al. (1984) and Forsberg and Puu (1984). The huge interest in high affinity irreversible inhibition is particularly apparent in the case of the wide family of irreversible inhibitors represented by compounds highly toxic for living organisms, such as pesticides and nerve gases that act primarily on acetylcholinesterases in the nervous system (Bajgar 2004).

Because of its great structural similarity with cholinesterase-like enzymes and proteins belonging to the α/β hydrolase superfamily, and in accordance with the evidence that also carboxylesterases from *Culex* mosquitoes, belonging to the same hormone sensitive lipase (HSL) family, was irreversibly inhibited by several acetylcholinesterase inhibitors (Karunaratne et al. 1993; Hemingway and Karunaratne 1998), EST2 from *A. acidocaldarius* is highly sensitive to the action of specific acetylcholinesterase inhibitors and in particular, to irreversible inhibitors (Manco et al. 1998).

Esterase 2 is a monomeric protein of about 34 KDa, which hydrolyses monoacyl esters of different acyl chain lengths and different compounds of pharmacological and industrial interest (Manco et al. 1998, 2002). The enzyme displays maximal activity on *p*-nitrophenyl (*p*NP) esters characterized by an acyl chain length of 6–8 carbon atoms, at an optimal temperature of 70°C. Furthermore, the EST2 three-dimensional structure has recently been solved at 2.6 Å (De Simone et al. 1999, 2000).

Biochemical and mutagenic studies allowed the identification of the residues involved in the reaction mechanism (Manco et al. 1999, 2001) that, similarly to that of serine proteases, can be subdivided into three steps, as described in Scheme 1: (1) formation of a tetrahedral intermediate TI1, by a nucleophilic attack of S155 on the carboxylic carbon atom of the ester substrate; (2) formation of an acyl-enzyme intermediate, by the release of a primary alcohol R-OH from TI1, as a consequence of proton transfer from H282, and the formation of a second tetrahedral intermediate TI2; (3) deacylation, through the nucleophilic attack of a water molecule thereby releasing the carboxylic acid and restoring the free enzyme.

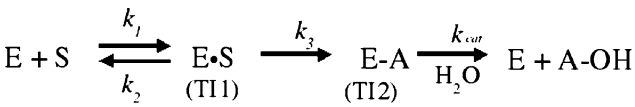

Scheme 1 Reaction mechanism of EST2 (see text)

Although, the solved three-dimensional structure of EST2 has revealed the fortuitous formation of a covalent adduct between the active site Ser-155 and a HEPES molecule (De Simone et al. 2000), prolonged incubations of EST2 in the presence of high concentrations of HEPES (up to 1 M) did not affect irreversibly the EST2 activity. From further analysis, was revealed that HEPES is a competitive inhibitor of the enzyme with a calculated K_i of 0.78 M (Manco et al. 2001).

In the present work, the irreversible inhibition of EST2 by the sulfonyl inhibitors phenylmethanesulfonyl fluoride (PMSF) and 1-hexadecanesulfonyl chloride (HDSC), as well as by the organophosphorous insecticide diethyl-*p*-

nitrophenyl phosphate (paraoxon), has been studied. The latter is an organophosphorus pesticide widely used in the agricultural field. Being only relatively degradable (Albero et al. 2003), paraoxon persists for a long time in the environment allowing its detection also in the food chain. Recently, it has been described as one of the most dangerous compounds for its toxic and cancerous effects on mammals (Cao et al. 1999; Carlson et al. 2000; Barber and Ehrich 2001; Abou-Donia 2003; Naravaneni and Jamil 2007), even at low concentrations (Sun et al. 2000; Saleh et al. 2003).

Experimental

Chemicals

All chemicals used in this study were of analytical grade and purchased from Sigma-Aldrich. The FPLC, chromatographic columns and SDS-PAGE molecular mass markers were purchased from Amersham Biosciences.

Enzyme preparation

EST2 was overexpressed in the mesophilic host *E. coli* strain BL21(DE3) and purified as previously described in Manco et al. (1998). The purity was tested by SDS-PAGE. The protein concentration was estimated by the optical absorbance at 280 nm, using a molar extinction coefficient of 1.34×10^5 M^{-1} cm^{-1} in 40 mM sodium phosphate buffer pH 7.1, at 25°C, as described in Manco et al. (1997).

Enzyme assay

The standard assay of esterase-catalyzed hydrolysis was carried out in 1.0 ml of a reaction mixture containing 40 mM sodium phosphate buffer, pH 7.1, 4% (v/v) acetonitrile, and 100 μM *p*-nitrophenyl-hexanoate (*p*NP-C6) as the substrate, by monitoring the increase of absorbance at 405 nm due to the release of 4-nitrophenolate (molar extinction coefficient of 13×10^3 M^{-1} cm^{-1}, at 405 nm) in a 1 cm path-length cell. The measurements were carried out in a double-beam Varian Cary 1E UV–Visible spectrophotometer (Varian, VIC, Australia), equipped with a temperature controller with Peltier effect with an error of 0.1°C, and by using an appropriate blank. An enzymatic unit was defined as the amount of enzyme that catalyzes the hydrolysis of 1 μmol of substrate in 1 min at 30°C.

Irreversible inhibition kinetic constants

Kinetic constant determination for PMSF, HDSC and paraoxon by time-dependent inactivation was carried out by incubating samples of EST2 (final concentrations, 0.97 μM) in 40 mM sodium phosphate buffer, pH 7.1 in the presence of different concentrations of inhibitor (final volume 0.5 ml). At each time interval, aliquots were removed from the inactivation mixture, opportunely diluted in 40 mM sodium phosphate buffer, pH 7.1, and immediately assayed in 1 ml of 100 μM *p*-NP-C6 dissolved in 40 mM sodium phosphate buffer, pH 7.1, 4% (v/v) acetonitrile at 30°C.

The rate constant at each inactivator concentration, k_{obs}, was determined by plotting the logarithm of the residual enzyme activity against time. K_i, the dissociation constant, and k_i, the rate constant for inactivation, were calculated by a non-linear regression fit (Grafit 5.0, Erithacus Software) of observed rate constants according to the following expression:

$$k_{obs} = \frac{k_i[I]}{K_i + [I]}. \quad (1)$$

Continuous monitoring of enzymatic activity in the presence of irreversible inhibitors was carried out in 1 cm path-length cells, containing in a final volume of 1 ml, 40 mM sodium phosphate buffer, pH 7.1, 100 μM *p*NP-C6 and inhibitor concentrations in the range 0.05–0.5 μM, 5.0–18.0 μM and 1.0–5.0 mM for paraoxon, HDSC and PMSF, respectively. After the addition of the enzyme (0.2 nM), the increase in absorbance at 405 nm was monitored at 30°C in a Varian Cary 1E UV–Visible spectrophotometer (Varian, VIC, Australia).

The apparent rate constants, A_c, were calculated by plotting the logarithm of the difference of product in the absence and presence of different inhibitor concentrations, against time. The values of the rate constant for inactivation (k_i) and dissociation (K_i), were calculated by the following expression:

$$A_c = \frac{k_i K_i}{1 + [S]/K_m + K_i[I]}. \quad (2)$$

All measures were carried out at least three times and the data analyzed by the software Grafit 5.0 (Erithacus Software).

Protection against inactivation

Samples of EST2 (0.57 μM) in buffer 40 mM sodium phosphate pH 7.1 were incubated in the presence of 5 μM HDSC at two different HEPES concentrations (2.0 and 4.0 mM). Alternatively, samples of EST2 (0.5 μM) in buffer 40 mM sodium phosphate pH 7.1 were incubated in the presence of 0.5 μM paraoxon or 100 μM PMSF, at several HEPES concentrations (from 4 to 40 mM). At each time interval, aliquots were withdrawn from the inactivation mixtures, and immediately assayed in 1 ml of 100 μM *p*NP-C6 in 40 mM sodium phosphate, pH 7.1, at 30°C.

All measurements were carried out at least three times and the data analyzed by the software Grafit 5.0 (Erithacus Software).

Inhibition of alternative catalytic site by HEPES

The inhibition on the alternative catalytic site was evaluated by assaying EST2 (0.2 nM) activity in the standard assays [40 mM sodium phosphate buffer, pH 7.1; 4% (v/v) acetonitrile] at 70°C in the presence of three different HEPES concentrations (0.1, 0.5 and 1 mM) and at different concentrations of *p*-nitrophenyl-dodecanoate (*p*NP-C12) (range 5–50 μM) as the substrate. For each HEPES concentration initial velocity versus substrate concentration data were fitted to the Lineweaver–Burk transformation of the Michaelis–Menten equation, by weighted linear least-squares analysis with a personal computer and the program Grafit 5.0 (Erithacus Software). Assays were done in duplicate or triplicate, and the results for kinetic data were the means of two independent experiments. The values of intercept on the vertical axis of the three measurements were replotted against the inhibitor concentration to obtain, from the intercept with the base axis, the value of the inhibition constant K_i.

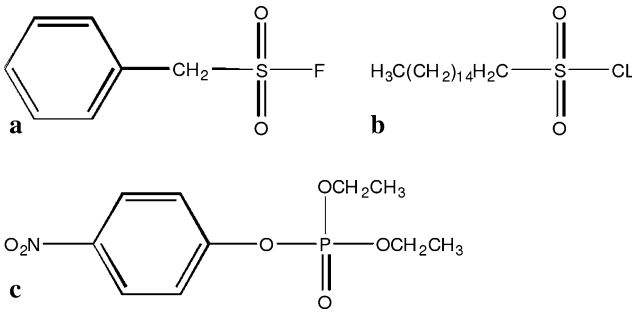

Fig. 1 Molecular formula. (*a*) PMSF, (*b*) HDSC and (*c*) paraoxon

Results and discussion

Kinetic analysis of EST2 inhibition by paraoxon, HDSC and PMSF

Esterase 2 is sensitive to the action of sulfonyl inhibitors such as aryl (PMSF) and alkyl (HDSC) derivatives (Fig. 1), which covalently react with the catalytic serine 155 in the enzyme active site (De Simone et al. 2004a) generating an analog of the second intermediate of the reaction pathway. The general mechanism of EST2 inhibition that can be proposed is shown in Scheme 2.

Scheme 2 Mechanism of inhibition/reactivation of EST2 (see text)

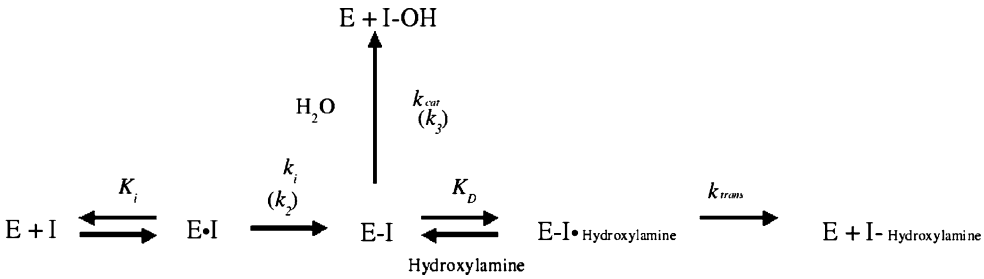

Reactivation experiments

Samples of EST2 (1.18 μM) in 40 mM sodium phosphate buffer, pH 7.1, were inhibited, either, in the presence of stoichiometric quantities of paraoxon, or of over-stoichiometric quantities of PMSF or HDSC. Full inactivation of EST2 by each inhibitor was confirmed by the standard enzymatic assay. Preliminarily, the excess of the inhibitor, in the samples of EST2 inhibited by PMSF and HDSC, was removed by a desalting gel filtration (G-25 Pharmacia Amersham Biosciences), and the enzyme concentration evaluated. Aqueous solutions of hydroxylamine, in the range of concentrations from 0.5 to 6 M, or alternatively, aqueous solutions of 2-(hydroxyiminomethyl)-1-methylpyridinium iodide (2-PAM) in the range from 0.001 to 0.3 M, were added to the different inactivated mixtures. The recovery of esterase activity was monitored by the standard assay for 48 h.

In agreement with the widely described reaction mechanism (De Simone et al. 2000, 2004b), the inhibition rate constant k_i corresponds to the acylation constant k_2, whereas k_3 represents the deacylation constant k_{cat} (compare with Scheme 1). Since, HDSC, PMSF and paraoxon act as irreversible inhibitors, the rate constant k_{cat} is very small.

Incubation of EST2 with HDSC resulted in time-dependent inactivation according to pseudo-first-order kinetics (Fig. 2a). The inactivation constant, K_{obs}, for each inhibitor concentration was obtained by plotting the natural logarithm of the residual enzyme activity versus time (Fig. 2b). A double-reciprocal re-plot of the pseudo-first-order rate constants against inhibitor concentration (Fig. 2d) yielded an inactivation rate constant k_i of 0.014 s^{-1} and a dissociation constant K_i of 0.36 μM (Table 1), in agreement with previously published data (De Simone et al. 2004b). The same measurements were carried out on PMSF applying the same

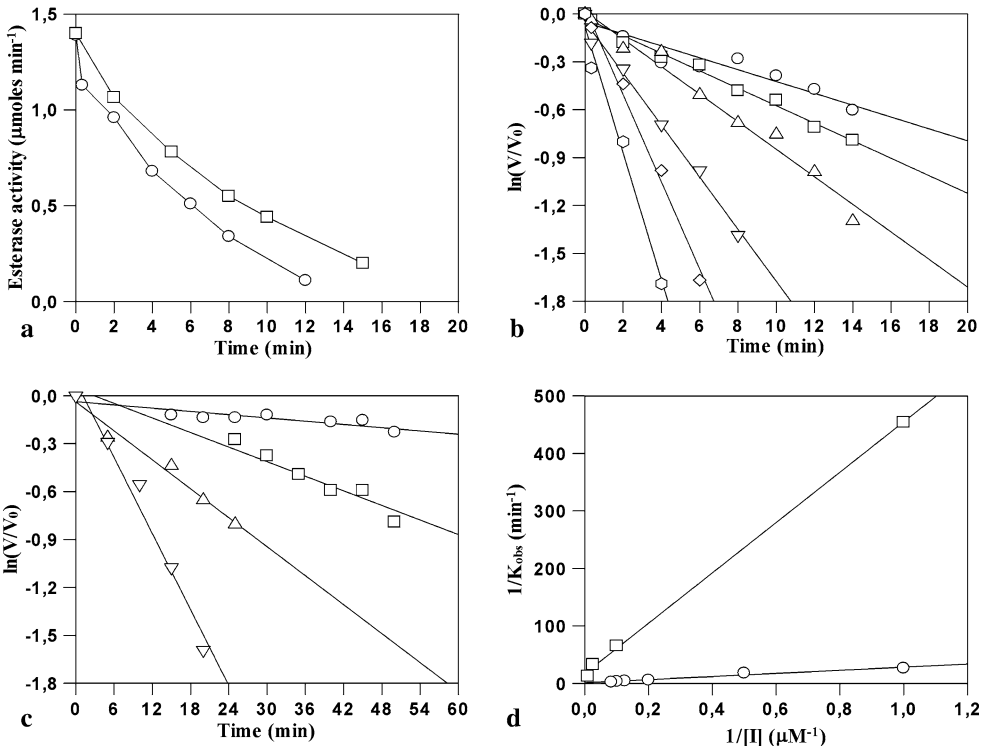

Fig. 2 Kinetic analysis of inhibition with HDSC and PMSF. **a** EST2 inactivation kinetic as function of time in the presence of 5 μM HDSC (*circle*) and 50 μM PMSF (*square*) inhibitors. **b** Logarithmic plot of EST2 residual activity against time at the following HDSC concentrations: 1 μM (*circle*), 2 μM (*square*), 5 μM (*triangle*), 8 μM (*inverse triangle*), 10 μM (*rhombus*), 12 μM (*hexagon*). **c** Logarithmic plot of EST2 residual activity against time at the following PMSF concentrations: 1 μM (*circle*), 10 μM (*square*), 40 μM (*triangle*), 100 μM (*inverse triangle*). **d** Double reciprocal plot of first-order rate constants taken from **b** and **c** against inhibitor concentrations, HDSC (*circle*) and PMSF (*square*)

Table 1 Kinetic parameters for the inactivation of EST2 by sulfonyl and organophosphorus inactivator using the pseudo first order plots

Complex E-I	K_i (μM)	k_i (10^{-3} s^{-1})	k_i/K_i (10^{-3} s^{-1} μM^{-1})
EST2 + HDSC	0.36 ± 0.032	14.0 ± 1.40	38.9
EST2 + PMSF	0.42 ± 0.039	0.96 ± 0.11	2.3
EST2 + paraoxon	ND	ND	ND

ND not determinable

kinetic treatment (Fig. 2c, d) thus obtaining an inactivation rate constant k_i of 0.96×10^{-3} s^{-1} and a dissociation constant K_i of 0.42 μM (Table 1).

The values of the kinetic constants of EST2 inactivation (Table 1) indicate a comparable affinity (K_i) of the two inhibitors towards EST2, but a different reactivity (k_i), yielding a greater specificity (k_i/K_i) of HDSC compared to PMSF. Since acyl chains over eight carbon atoms of the substrate (or inhibitor), such as HDSC, bind into a different pocket (De Simone et al. 2004b), it is consequential to speculate that the different specificity observed for the two sulfonyl inhibitors reflects the two different binding modes in the catalytic pocket. However, the EST2 specificity towards substrates having acyl chains of six to eight carbon atoms is greater than towards substrates having acyl chains over eight carbon atoms (De Simone et al. 2004b), and therefore we cannot exclude the possibility that the aryl chain and/or the fluorine atom in the PMSF molecule play a role in the reduced reactivity of organic sulfur.

The inactivation process of EST2 by the organophosphorous inhibitor (paraoxon) (Fig. 1), cannot be described as pseudo-first-order kinetics in contrast to the sulfonyl inhibitors. Actually, the loss in activity, measured immediately after the addition of the inhibitor, corresponds exactly to the amount of enzyme that can be inhibited by the paraoxon added (data not shown). These results indicate that the inhibition reaction is completed in a few seconds, making impracticable standard assay measurements and suggesting high-affinity inhibition kinetics.

The continuous monitoring of the enzymatic reaction in the presence of the inhibitor allowed us to obtain the apparent rate constants for high-affinity inhibition kinetics (Liu and Tsou 1986), like those observed for EST2 in the presence of paraoxon. When both the substrate and the irreversible inhibitor are simultaneously present, the time course of product formation can be described according to Eq. (3):

$$[P] = [P]_{\infty}\left(1 - e^{A_c[I]t}\right) \quad (3)$$

where $[P]$ and $[P]_{\infty}$ represent the concentrations of product formed at time t and when t approaches infinity, respectively, A_c is the apparent rate constant for the formation of the inhibited enzyme and $[I]$ the concentration of the inhibitor (Tian and Tsou 1982). Both $[S]$ and $[I]$ have to be much greater than $[E]$ as an essential condition (Liu and Tsou 1986). The time-course of product formation during the inhibition of esterase activity by paraoxon with

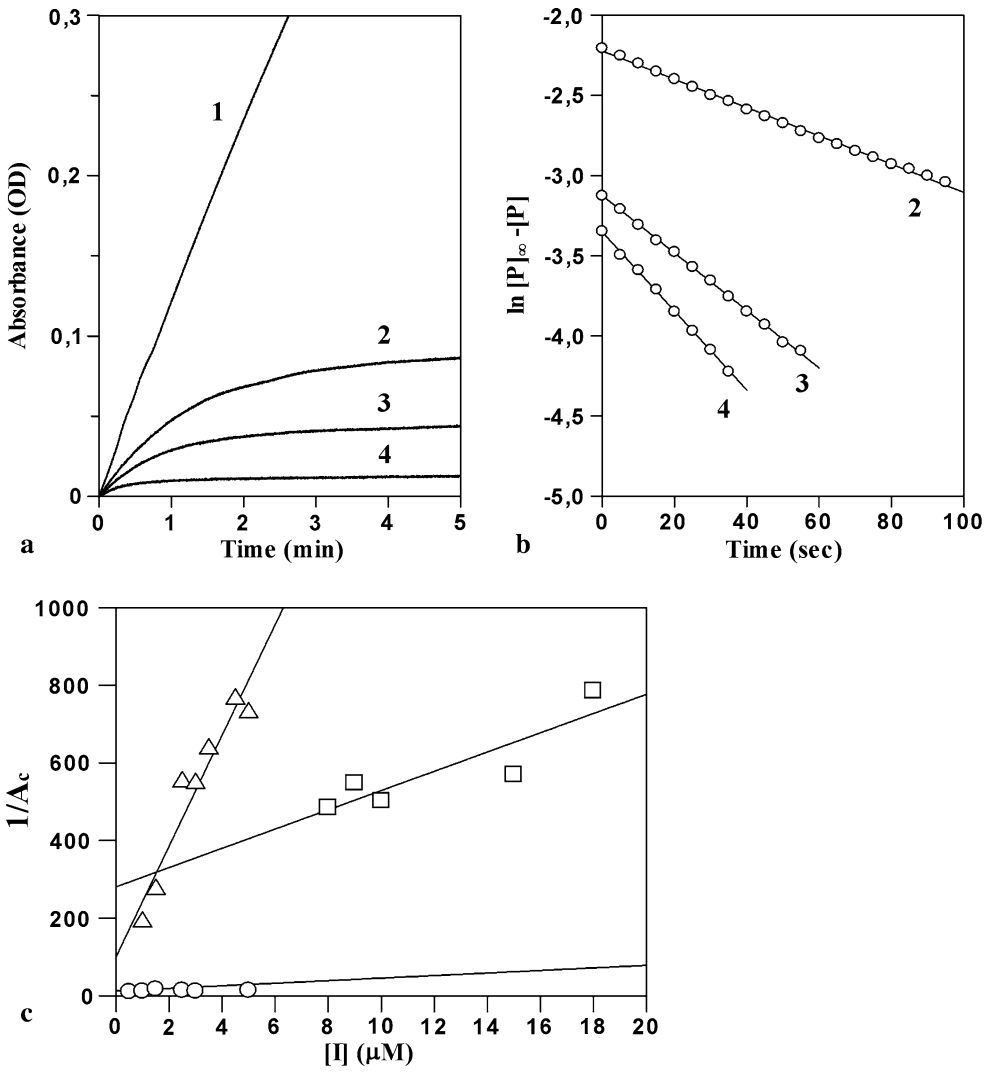

Fig. 3 High-affinity inhibition analysis. **a** Time-course of *p*NP formation in the esterase assay at different paraoxon concentrations: 0.0 μM (1); 0.15 μM (2); 0.25 μM (3); 0.5 μM (4). **b** Semi-logarithmic plots for the determination of the apparent rate constants of inhibition; data taken from **a**. **c** Reciprocal plot of ln(A_c) against inhibitor concentrations for paraoxon (*circle*), HDSC (*square*), PMSF (*triangle*). Paraoxon concentration units have to be considered as multiplied by 10^{-3}

*p*NP-C6 as a substrate (Fig. 3a) is in agreement with Eq. 3, which predicts that $[P]$ approaches a constant value, $[P]_\infty$, when t approaches infinity and $[P]_\infty$ decreases with increasing $[I]$. Plots of ln $[P]_\infty - [P]$ against t should give straight lines with slopes of A_c $[I]$ (Fig. 3b), according to the Eq. (4):

$$\ln\left([P]_\infty - [P]\right) = \ln[P]_\infty - A_c[I]t. \quad (4)$$

Since $[I]$ is known, the apparent rate constant can then be obtained from the slopes of the straight lines.

It is known that some inhibitors combine reversibly with the enzyme before forming an irreversible complex (Scheme 3).

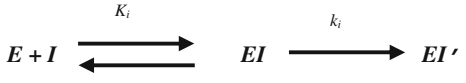

Scheme 3 General mechanism of irreversible inhibition (see text)

In such cases of complex competitive inhibition, the dependency of the apparent rate constant, A_c, on both $[S]$ and $[I]$, has been shown (Tian and Tsou 1982), as described in Eq. (5):

$$A_c = \frac{k_i K_i}{1 + [S]/K_m + K_i[I]}. \quad (5)$$

Since the Michaelis constant is known, the values of k_i and K_i can be calculated either by the slopes and intercepts of $1/A_c$ versus 1/[S] or alternatively by $1/A_c$ versus $1/[I]$ or $1/A_c[I]$ versus $1/[I]$ (Fig. 3c).

The calculated parameters (Table 2) indicate an apparent rate constant (k_i) of 304.0 10^{-3} s^{-1}, an apparent affinity constant of inhibition (K_i) of 1.8 μM and an inhibition specificity (k_i/K_i) of 169.0 μM^{-1} s^{-1}.

In order to compare these results with the kinetic parameters for the other inhibitors, the same analysis, with the same substrate, was carried out by using HDSC and PMSF (Fig. 3c) and the results are reported in Table 2. The

Table 2 Kinetic parameters for the inactivation of EST2 by sulfonyl and organophosphorus inactivators using the continuous monitoring of the enzymatic reaction in the presence of inhibitor

Complex E-I	K_i (μM)	k_i (10^{-3} s^{-1})	k_i/K_i (10^{-3} s^{-1} μM^{-1})
EST2 + HDSC	0.64 ± 0.19	40.3 ± 8.3	62.9
EST2 + PMSF	10380.0 ± 1353.7	7.0 ± 1.1	6.74×10^{-4}
EST2 + paraoxon	1.8 ± 0.53	304.0 ± 59.1	169.0

kinetic parameters measured for HDSC are similar to those obtained in the pseudo-first order approach, in agreement with the binding of this inhibitor to an EST2 alternative binding site (De Simone et al. 2004b). On the other hand, PMSF affinity for the enzyme decreased about 20,000 times (see K_i values in Tables 1 and 2), according to a kinetic competition of the inhibitor for the canonical substrate site, where the *p*NP-exanoate acyl chain normally binds. Because of these observations, the measured apparent kinetic value K_i for paraoxon, which should interact at the same substrate site, is predicted to be a thousand times lower, thus suggesting a very high affinity between EST2 and this inhibitor.

The study of EST2 irreversible inhibition shown here gives us useful information about the behavior of this enzyme, and in general of other bacterial enzymes of the HSL family. The analysis of apparent inhibition constants indicates that the key role in the inhibition kinetics of EST2 should not be ascribed to the chemical nature of the bound group (alkyl or aryl) of the inhibitor, considering that in the experiments of pseudo-first-order kinetics, the affinity for PMSF and HDSC was revealed to be similar (Table 1). Instead, in the experiments of continuous monitoring of the substrate reaction in the presence of the inhibitor, the kinetic constant values for PMSF and paraoxon were revealed to be remarkably different. From a structural analysis of the corresponding molecular formula (Fig. 1) it can be observed that, although it shows a similar structure, we are dealing with a phosphonate for the paraoxon and a sulfonate for the PMSF. Furthermore, in one case, we have the bad leaving group fluoride (a strong base) and, in the other, the good one *p*NP (a weak base). Therefore, we can assume that these differences contribute, in a determining way, to the greater specificity of EST2 towards the paraoxon. In other words the phosphonate is much more reactive than the sulfonate towards the serine nucleophilic attack.

In conclusion, a survey of the literature seems to indicate that the apparent inhibitor specificity constant (k_i/K_i) of EST2 is similar to or higher than (by about 4 times) those of other acetylcholinesterases from different sources and determined by the same approach (Liu and Tsou 1986), as well as within the limits of these determination techniques, higher than those measured for esterases from *Culex* mosquitoes (Karunaratne et al. 1993; Small et al. 1999).

Protection against irreversible inhibition and analysis of the competitive inhibition of alternative catalytic site by HEPES

Although the solved three-dimensional structure of EST2 has revealed the fortuitous formation of a covalent adduct (surely due to the peculiarity of crystallization conditions) between the active site Ser-155 and a HEPES molecule (De Simone et al. 2000), high concentrations of HEPES (up to 1 M) and prolonged incubations of EST2 with HEPES, did not affect irreversibly the EST2 activity at saturating concentrations of substrate *p*NP-C6. From this analysis, it was revealed that HEPES is a poor competitive inhibitor of the enzyme with a calculated K_i of 0.78 M (Manco et al. 2001).

Anyway, the direct indication that HEPES interacts with the catalytic EST2 site, as a competitive inhibitor, was useful in a study of active site protection from irreversible inhibition. If an irreversible inhibitor acts by binding to a group at the active site, the presence of a competitive inhibitor will protect against inhibition by slowing down the rate at which irreversible inhibition occurs. This protective effect may be used as good evidence of a specific reaction of the irreversible inhibitor with the active site (Dixon and Webb 1979).

Besides, a therapeutic efficacy of reversible inhibitors on the acetylcholinesterase irreversible inhibition by paraoxon has recently been reported. This study has indicated that the residual acetylcholinesterase activity is significantly higher in the presence of reversibly blocking agents, and after discontinuing paraoxon, the activity increased even in the presence of reversible blockers. Finally, stopping the delivery of the reversible blocking agents resulted in a 10–35% recovery of the enzyme activity, suggesting potential applications of these inhibitors (Eckert et al. 2006).

Protection of EST2 activity against HDSC, PMSF and paraoxon irreversible inhibition was performed by incubating the enzyme in the presence of different HEPES concentrations at increasing concentrations of the irreversible inhibitor.

Due to the low affinity of HEPES for the EST2 catalytic site, protection from inactivation using PMSF and paraoxon was not observed (data not shown), in agreement with the high affinity shown by these irreversible inhibitors

(Tables 1, 2, respectively). Unexpectedly, a protective effect of HEPES on EST2 irreversible inhibition by HDSC was observed (Fig. 4a), suggesting that HEPES could interact in some way with the secondary binding pocket of the enzyme, and above all with better affinity.

In order to clarify the interaction between HDSC and HEPES, we performed an inhibition study on the alternative catalytic site, by assaying EST2 activity in the presence of different HEPES concentrations and using *p*NP-C12 as the substrate. The plot of the inverse of V_{max} versus the inverse of substrate concentration (Fig. 4b) indicated a non-competitive inhibition of HEPES on *p*NP-C12, reducing the maximum rate of reaction without changing the apparent binding constant of the enzyme for the substrate. Usually, in a non-competitive inhibition the inhibitor binds to the enzyme at a site other than the enzyme's active site, causing a change in the structure and shape of the enzyme that is no longer able to bind with a substrate correctly, and therefore affecting the rate of the reaction. Although HEPES engagement at the same time and in both acyl-binding pockets is the most obvious explanation for the experimental results, the huge difference in affinity between the irreversible and reversible inhibitors leads to a second hypothesis, namely that the entrance of HEPES in the primary pocket causes structural modifications that prevent the access of HDSC to the second pocket. This hypothesis could suggest a possible cross talk between sites. In this case it is worth noting that the HEPES and HDSC binding sites partially overlap and that molecules compete for the same nucleophilic serine.

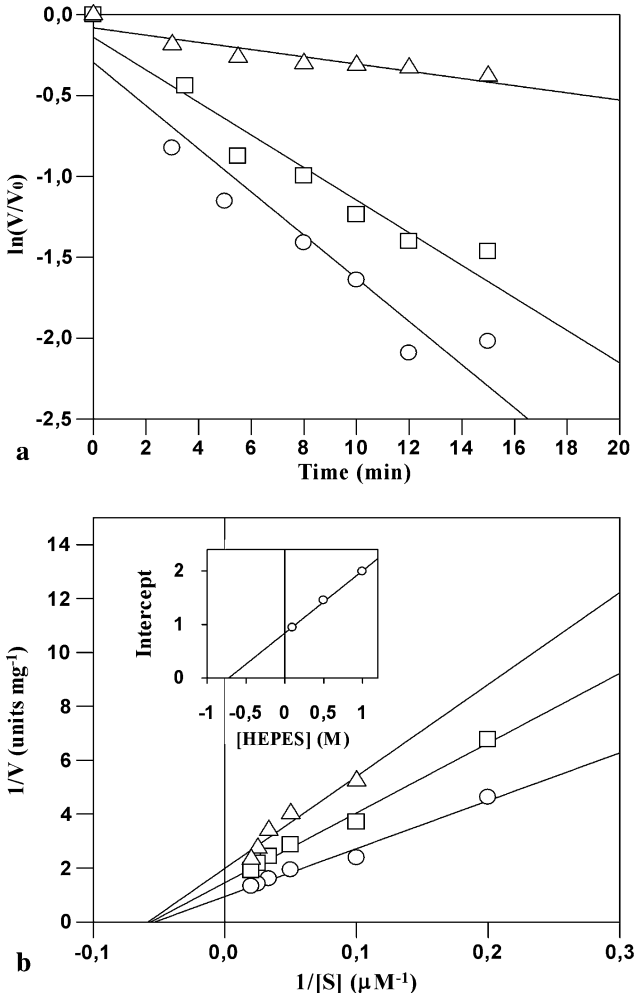

Fig. 4 EST2 reversible inhibition and protection against inactivation by HEPES. **a** Protective effect of different HEPES concentrations on EST2 inhibited with 5 µM HDSC. Without HEPES (*circle*), 2 mM HEPES (*square*), 4 mM HEPES (*triangle*). **b** Lineweaver–Burk plot of EST2 activity measured in the concentration range 5–50 µM of *p*NP-dodecanoate in the presence of 0.1 (*circle*), 0.5 (*square*) and 1 (*triangle*) mM HEPES, at 70°C. In the *inset*, the intercepts of the three lines with the vertical axis were replotted against the inhibitor concentrations

In conclusion, HEPES exerts a dual reversible inhibition role: competitive against *p*NP-C6 and non-competitive against *p*NP-C12. This observation makes it clear that knowledge of the inhibitor location in the catalytic pocket of the enzyme is pivotal in order to carry out an accurate kinetic analysis, and suggest interesting new questions on active site mechanisms of regulation analogous to allosteric modulation, and so encouraging new investigations.

Reactivation

As described in Scheme 2, during the inhibition process, it is possible to remove the inhibitor bound to the active site catalytic residue by a nucleophile stronger than water. Hydroxylamine, described in literature as a reagent for recovering catalytic activity after irreversible inhibition (Vilanova and Vicedo 1983; Pyatakova et al. 1999), and 2-PAM, developed as an antidote to chemical warfare agents and organophosphorous insecticides (Worek et al. 1996), have been used here as re-activators of the EST2-paraoxon inactive complex. After 5 min incubation, a 90% recovery of the esterase activity in the presence of 5 M hydroxylamine was observed (Fig. 5). No further recovery of activity was observed even after 24 h incubation in the presence of hydroxylamine (data not shown). These results indicate that such a substance could be employed as a re-activator of the inactive complex EST2-paraoxon.

Ineffective results were obtained using 2-PAM as re-activator. In fact, samples of the EST2/paraoxon inactive complex treated with 2-PAM at concentrations up to 0.15 M and for an incubation time up to 48 h did not show any recovery of activity, even if it is important to emphasize that this re-activator was employed at lower molar concentrations than that of hydroxylamine, due to its limited solubility in water.

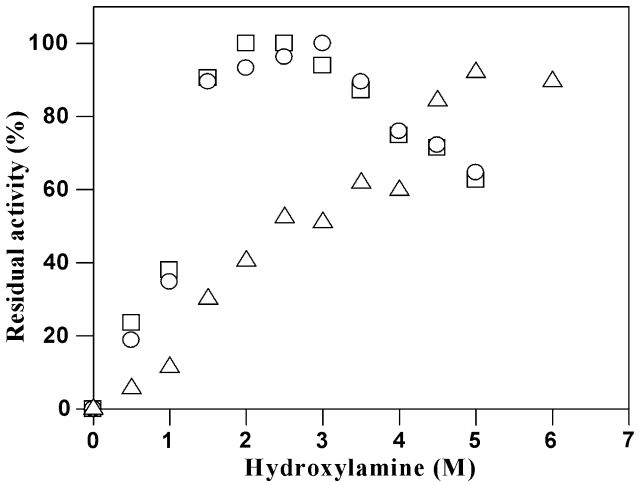

Fig. 5 Inhibited-EST2 reactivation by hydroxylamine. Reactivation of paraoxon-inhibited EST2 (*triangle*) after 5 min incubation with different concentrations of hydroxylamine hydrochloride ranging from 0 to 6 M. Reactivation of HDSC (*square*) and PMSF (*circle*) inhibited EST2 after 20 min incubation with different concentrations of hydroxylamine hydrochloride in the range 0–5 M. The data are normalized as function of hydroxylamine effects on enzymatic activity

A reactivation of the enzyme/sulfonate inhibited complex was observed at lower concentrations of hydroxylamine compared to the concentrations used for the reactivation of the enzyme/paraoxon complex (Fig. 5), thus suggesting a lesser stability for the EST2 complex with sulfonates in comparison to organophosphates.

Conclusions

With regard to the susceptibility of EST2 to paraoxon, we have described here for the first time high-affinity kinetics for a thermostable bacterial esterase belonging to the HSL family. Above all, we have demonstrated a higher sensitivity of an esterase from an extremophilic eubacterium towards compounds, until now described in detail only in term of its effect on insect acetylcholinesterases and carboxylesterases (Forsberg and Puu 1984; Liu and Tsou 1986; Hemingway and Karunaratne 1998; Zdrazilová et al. 2006). These observations suggest interesting questions on evolution and biodiversity, since the involvement of the mosquito carboxylesterases in resistance to pesticides by sequestration followed by the slow turnover is clear, whereas the high reactivity showed by a bacterial carboxylesterase against paraoxon remains to be clarified.

Finally, given the necessity of removing such molecules from the environment, but also of measuring the levels of contamination, the employment of thermostable EST2 as a biosensor for pesticides (and chemical warfare agents) is promising, in contrast to the usually used free or immobilized forms of less stable acetylcholinesterases (Mionetto et al. 1994; Bernabei et al. 1993; Cremisini et al. 1995). Exploitation of EST2 could bring remarkable advantages, such as stability to other harsh conditions, possibility of obtaining large amounts of enzyme at a low cost, remarkable sensitivity and specificity, low interference from other compounds, and the possibility of biosensor recovery.

References

Abou-Donia MB (2003) Organophosphorus ester-induced chronic neurotoxicity. Arch Environ Health 58:484–497

Albero B, Sanchez-Brunete C, Tadeo JL (2003) Determination of organophosphorus pesticides in fruit juices by matrix solid-phase dispersion and gas chromatography. J Agric Food Chem 51:6915–6921

Bajgar J (2004) Organophosphates/nerve agent poisoning: mechanism of action, diagnosis, prophylaxis, and treatment. Adv Clin Chem 38:151–216

Barber DS, Ehrich M (2001) Esterase inhibition in SH-SY5Y human neuroblastoma cells following exposure to organophosphorus compounds for 28 days. In Vitr Mol Toxicol 14:129–135

Bernabei M, Chiavarini S, Cremisini C, Palleschi G (1993) Anticholinesterase activity measurement by a choline biosensor: application in water analysis. Biosens Bioelectron 8:265–271

Bhat JY, Shastri BG, Balaram H (2008) Kinetic and biochemical characterization of *Plasmodium falciparum* GMP synthetase. Biochem J 409:263–273

Cao CJ, Mioduszewski RJ, Menking DE, Valdes JJ, Katz EJ, Eldefrawi ME, Eldefrawi AT (1999) Cytotoxicity of organophosphate anticholinesterases. In Vitro Cell Dev Biol Anim 35:493–500

Carlson K, Jortner BS, Ehrich M (2000) Organophosphorus compound-induced apoptosis in SH-SY5Y human neuroblastoma cells. Toxicol Appl Pharmacol 168:102–113

Cremisini C, Di Sario S, Mela J, Pilloton R, Palleschi G (1995) Evaluation of the use of free and immobilised acetylcholinesterase for paraoxon detection with an amperometric choline oxidase based biosensor. Anal Chim Acta 311:273–280

Demo SD, Kirk CJ, Aujay MA, Buchholz TJ, Dajee M, Ho MN, Jiang J, Laidig GJ, Lewis ER, Parlati F, Shenk KD, Smyth MS, Sun CM, Vallone MK, Woo TM, Molineaux CJ, Bennett MK (2007) Antitumor activity of PR-171, a novel irreversible inhibitor of the proteasome. Cancer Res 67:6383–6391

De Simone G, Manco G, Galdiero S, Lombardi A, Rossi M, Pavone V (1999) Crystallization and preliminary X-ray diffraction studies of the carboxylesterase EST2 from *Alicyclobacillus acidocaldarius*. Acta Crystallogr D Biol Crystallogr 55:1348–1349

De Simone G, Galdiero S, Manco G, Lang D, Rossi M, Pedone C (2000) A snapshot of a transition state analogue of a novel thermophilic esterase belonging to the subfamily of mammalian hormone-sensitive lipase. J Mol Biol 303:761–771

De Simone G, Menchise V, Alterio V, Mandrich L, Rossi M, Manco G, Pedone C (2004a) The crystal structure of an EST2 mutant unveils structural insights on the H group of the carboxylesterase/lipase family. J Mol Biol 343:137–146

De Simone G, Mandrich L, Menchise V, Giordano V, Febbraio F, Rossi M, Pedone C, Manco G (2004b) A substrate-induced switch in the reaction mechanism of a thermophilic esterase: kinetic evidences and structural basis. J Biol Chem 279:6815–6823

Dixon M, Webb EC (1979) Enzymes, 3rd edn. Academic Press, New York

Eckert S, Eyer P, MÜckter H, Worek F (2006) Kinetic analysis of the protection afforded by reversible inhibitors against irreversible inhibition of acetylcholinesterase by highly toxic organophosphorus compounds. Biochem Pharmacol 72:344–357

Febbraio F, Barone R, D'Auria S, Rossi M, Nucci R, Piccialli G, De Napoli L, Orru S, Pucci P (1997) Identification of the active site nucleophile in the thermostable β-glycosidase from the archaeon *Sulfolobus solfataricus* expressed in *Escherichia coli*. Biochemistry 36:3068–3075

Forsberg A, Puu G (1984) Kinetics for the inhibition of acetylcholinesterase from the electric eel by some organophosphates and carbamates. Eur J Biochem 140:153–156

Hemingway J, Karunaratne SH (1998) Mosquito carboxylesterases: a review of the molecular biology and biochemistry of a major insecticide resistance mechanism. Med Vet Entomol 12:1–12

Hugonnet JE, Blanchard JS (2007) Irreversible inhibition of the *Mycobacterium tuberculosis* beta-lactamase by clavulanate. Biochemistry 46:11998–12004

Karunaratne SH, Jayawardena KG, Hemingway J, Ketterman AJ (1993) Characterization of a B-type esterase involved in insecticide resistance from the mosquito *Culex quinquefasciatus*. Biochem J 294:575–579

Legler G, Harder A (1978) Amino acid sequence at the active site of β-glucosidase A from bitter almonds. Biochim Biophys Acta 524:102–108

Leytus SP, Toledo DL, Mangel WF (1984) Theory and experimental method for determining individual kinetic constants of fast-acting, irreversible proteinase inhibitors. Biochim Biophys Acta 788:74–86

Liu W, Tsou CL (1986) Determination of rate constants for the irreversible inhibition of acetylcholine esterase by continuously monitoring the substrate reaction in the presence of the inhibitor. Biochim Biophys Acta 870:185–190

Lu J, Chew EH, Holmgren A (2007) Targeting thioredoxin reductase is a basis for cancer therapy by arsenic trioxide. Proc Natl Acad Sci USA 104:12288–12293

Maklakov A, Ishaaya I, Freidberg A, Yawetz A, Horowitz AR, Yarom I (2001) Toxicological studies of organophosphate and pyrethroid insecticides for controlling the fruit fly *Dacus ciliatus* (Diptera: Tephritidae). J Econ Entomol 94:1059–1066

Manco G, Adinolfi E, Pisani FM, Carratore V, Rossi M (1997) Identification of an esterase from *Bacillus acidocaldarius* with sequence similarity to a hormone sensitive lipase subfamily. Pept Lett 4:375–382

Manco G, Adinolfi E, Pisani FM, Ottolina G, Carrea G, Rossi M (1998) Overexpression and properties of a new thermophilic and thermostable esterase from *Bacillus acidocaldarius* with sequence similarity to hormone sensitive lipase subfamily. Biochem J 332:203–212

Manco G, Febbraio F, Adinolfi E, Rossi M (1999) Homology modeling and active site residues probing of the thermophilic *Alicyclobacillus acidocaldarius* esterase 2. Prot Sci 8:1789–1796

Manco G, Mandrich L, Rossi M (2001) Residues at the active site of the esterase 2 from *Alicyclobacillus acidocaldarius* involved in substrate specificity and catalytic activity at high temperature. J Biol Chem 276:37482–37490

Manco G, Carrea G, Giosue E, Ottolina G, Adamo G, Rossi M (2002) Modification of the enantioselectivity of two homologous thermophilic carboxylesterases from *Alicyclobacillus acidocaldarius* and *Archaeoglobus fulgidus* by random mutagenesis and screening. Extremophiles 6:325–331

Mionetto N, Marty JL, Karube I (1994) Acetylcholinesterase in organic solvents for the detection of pesticides: biosensor application. Biosens Bioelectron 9:463–470

Naravaneni R, Jamil K (2007) Determination of AChE levels and genotoxic effects in farmers occupationally exposed to pesticides. Hum Exp Toxicol 26:723–731

Pyatakova NV, Grigoryev NB, Severina IS (1999) Role of soluble guanylate cyclase in reactivation of choline esterase inhibited by phosphoorganic compounds. Biochemistry (Mosc) 64:91–94

Saleh AM, Vijayasarathy C, Fernandez-Cabezudo M, Taleb M, Petroianu G (2003) Influence of paraoxon (POX) and parathion (PAT) on apoptosis: a possible mechanism for toxicity in low-dose exposure. J Appl Toxicol 23:23–29

Small GJ, Karunaratne SH, Chadee DD, Hemingway J (1999) Molecular and kinetic evidence for allelic variants of esterase Estβ1 in the mosquito *Culex quinquefasciatus*. Med Vet Entomol 13:274–281

Sun X, Liu XB, Martinez JR, Zhang GH (2000) Effects of low concentrations of paraoxon on Ca(2+) mobilization in a human parotid salivary cell-line HSY. Arch Oral Biol 45:621–638

Tian WX, Tsou CL (1982) Determination of the rate constant of enzyme modification by measuring the substrate reaction in the presence of the modifier. Biochemistry 21:1028–1032

Tull D, Withers SG, Gilkes NR, Kilburn DG, Warren RA, Aebersold R (1991) Glutamic acid 274 is the nucleophile in the active site of a "retaining" exoglucanase from *Cellulomonas fimi*. J Biol Chem 266:15621–15625

Vilanova E, Vicedo JL (1983) Serum cholinesterase inhibitors in the commercial hexane impurities. Arch Toxicol 53:59–69

Withers SG, Aebersold R (1995) Approaches to labeling and identification of active site residues in glycosidases. Prot Sci 4:361–372

Worek F, Kirchner T, Backer M, Szinicz L (1996) Reactivation by various oximes of human erythrocyte acetylcholinesterase inhibited by different organophosphorus compounds. Arch Toxicol 70:497–503

Zdrazilová P, Stěpánková S, Komersová A, Vránová M, Komers K, Cegan A (2006) Kinetics of 13 new cholinesterase inhibitors. Z Naturforsch [C] 61:611–617